Metrol. Meas. Syst., Vol. XIX (2012), No.1, pp. 159–168.

PAN POLSKA AKADEMIA NAUK

METROLOGY AND MEASUREMENT SYSTEMS

Index 330930, ISSN 0860-8229

www.metrology.pg.gda.pl

M&MS

LOW VOLTAGE INTEGRATED CONVERTER FOR WASTE HEAT THEREMOELECTRIC HARVESTERS

Piotr Dziurdzia, Mariusz Mysiura, Adam Gołda

AGH University of Science and Technology, Al. Mickiewicza 30, 30-059 Kraków, Poland (✉ Piotr.Dziurdzia@agh.edu.pl)

Abstract

The paper deals with an application-specific integrated circuit (ASIC) facilitating voltage conversion in thermoelectric energy harvesters. The chip is intended to be used to boost up the voltage coming from a thermoelectric module to a level that is required by electronic circuits constituting wireless sensor nodes. The designed charge pump does not need any external parts for its proper operation because all the capacitors, switches and oscillator are integrated on the common silicon die. The topography of the main functional blocks and post-layout simulations of the designed integrated circuit are shown in the article.

Keywords: charge pump, DC-DC conversion, thermoelectric conversion, energy harvesting.

1. Introduction

Energy harvesting technologies that utilize some small pieces of free ambient energy in the form of light, vibrations and heat are playing a more and more important role in many domains. Replacing power mains cables or batteries by quite autonomous sources of energy scavenging heat from human warmth or industrial vibrations appeared to be very promising solutions in emerging applications coming from the biomedical industry, military, aerospace, etc. [1, 2].

For some years the authors have dealt with thermogenerators based on Peltier modules that could harvest waste industrial heat and convert it into electrical energy that is next used to supply nodes of wireless sensor networks (WSN) [3, 4]. In thermoelectric generators the output voltage is approximately proportional to the temperature gradient but its level is mostly not sufficient to be directly used to supply sensor nodes. Therefore different low voltage solutions have to be used to increase the voltage to a level required by microelectronic circuits [5, 6].

So far, charge pumps were commonly used in low voltage applications where supply voltages were insufficient to perform some specific operations, for instance in nonvolatile EEPROM and flash memories, LCD and LED controllers, digital level interfaces, integrated systems on chips (SoC) for supplying analogue parts, etc. [7-9]. Lastly, integrated charge pumps are becoming more and more popular also in emerging energy harvesting technologies and they are used to boost up voltages to levels required by microcontrollers, sensors and transceivers.

Most of the integrated low DC-DC voltage boosting circuits are based on the Dickson charge pump in which diodes were replaced with MOS transistors working in a diode mode, as shown in Fig. 1 [10, 11]. The total charge that is transported to the output of the M-stage Dickson charge pump can be expressed as in (1).

Article history: received on Nov. 2, 2011; accepted on Jan. 10, 2012; available online on March 12, 2012.

$$Q_M = \sum_{i=1}^{M-1} \frac{1}{2} C(i)^2 V_{IN} = \frac{M(M+1)(M+2)}{12} CV_{IN} \tag{1}$$

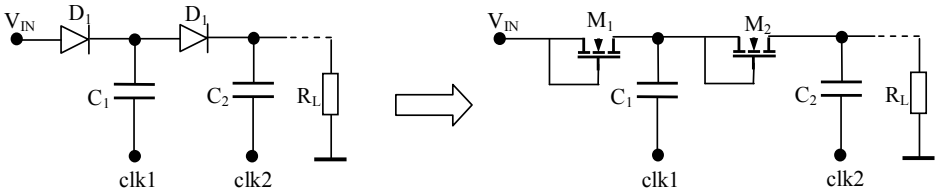

Fig. 1. Dickson charge pump based on diodes and NMOS transistors working in a diode mode.

In comparison with a classical circuit of a charge pump made of N voltage doublers [12], the pumped output charge can be calculated as in (2). Starting from the seventh stage, the Dickson charge pump manifests better charge pumping efficiency η (3), (Fig. 2). But due to the fact that it has a simpler structure it is more convenient for integration, therefore it is commonly used also in applications with only a few pump stages.

$$Q_N = \sum_{i=1}^{N} \frac{C}{2} \left[\left(2^i\right)^2 V_{IN} + \left(2^{i-1}\right)^2 V_{IN} \right] = \frac{5\left(N^2-1\right)}{6} CV_{IN} \tag{2}$$

$$\eta = \frac{Q_M}{Q_N} = \frac{M(M+2)}{10(M-1)} \tag{3}$$

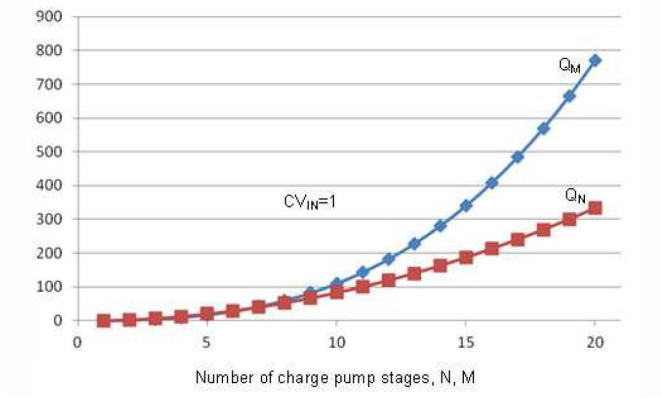

Fig. 2. Total charge transferred to the output of a classical voltage doubler Q_N and Dickson charge pump Q_M against the number of charge pumping stages.

In the paper an application-specific integrated circuit (ASIC) is presented. It is intended to be used for energy conversion coming from thermoelectric generators (TEGs), working at relatively high temperatures reaching up to 100°C.

The ASIC supports thermoelectric conversion in the TEG by transforming low voltage levels into single volts that are sufficient to supply a wireless sensor node (WSN) (Fig. 3). The TEG utilizes the Seebeck voltage resulting from a temperature gradient ΔT existing between two plates of a Peltier module. The obtained voltage levels are then transferred and

amplified by a Dickson CMOS charge pump that was realized in the form of a specific integrated circuit.

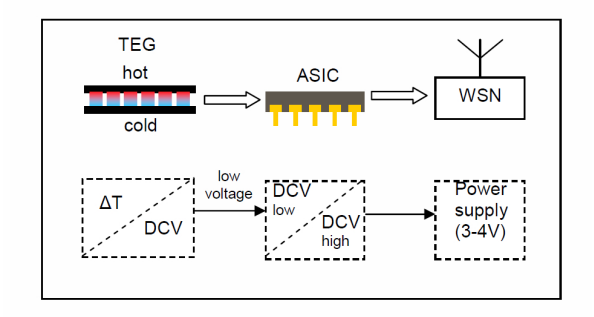

Fig. 3. A block diagram of thermoelectric conversion supported by a charge pump (ASIC).

2. Integrated circuit design

Our objective was to design a DC voltage converter circuit by modeling transistor dimensions in CMOS 180nm technology in a way to meet the preliminary assumptions saying that: for an input voltage about 1V the circuit should provide an output voltage level more than 3V and an output load current of at least 100μA. Apart from the charge pump, the ASIC should consist of a ring oscillator, switches and capacitors realized in CMOS technology and integrated on a common silicon die, so that no external elements were needed in order to increase voltage levels.

2.1. Charge pump

In our solution the DC/DC converter is based on a modified Dickson charge pump that was presented by Ahmadi and Jullien in [13], in which pMOS transistors working in a diode mode were playing the role of switches. The three-stage charge pump is shown in Fig. 4.

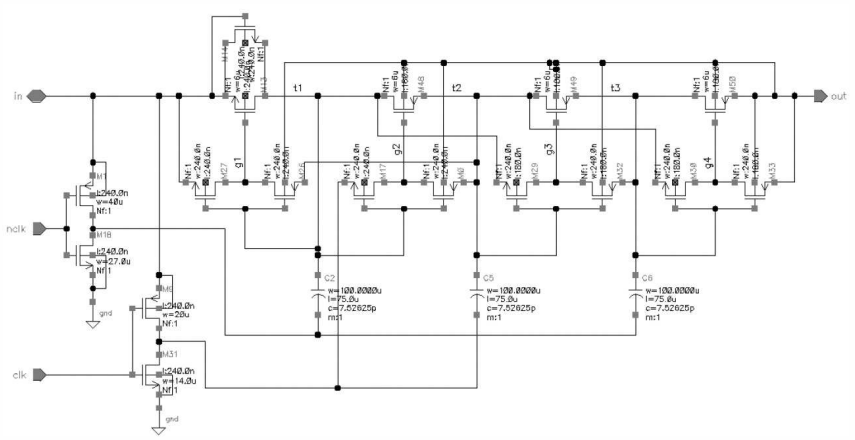

Fig. 4. Scheme of the three-stage charge pump.

The conducting PMOS transistors ensure much lower voltage drop on the way of charge transfer in comparison with the classical Dickson charge pump with diodes. Moreover, in the

presented circuit the body effect impact on increasing the threshold voltage was minimized. Therefore the output voltage of the charge pump was not affected by the increasing number of stages to a large extent. Additionally, each section of the charge pump was controlled by a dynamic inverter. Low and high levels of the inverters were changing in the course of the clock signals and they depended on the voltage levels at the other sections.

In the course of modeling, some simulations were performed in order to set the proper channel width of the switching transistors. From the graphs shown in Fig. 5 it is evident that the output voltage is saturated around 3V for the channel width larger than 5µm. Therefore the optimal value was chosen for W=6µm. Larger dimensions of transistors would not improve the level of the output voltage significantly, even would worsen the performance of the charge pump by introducing additional parasitic capacitances.

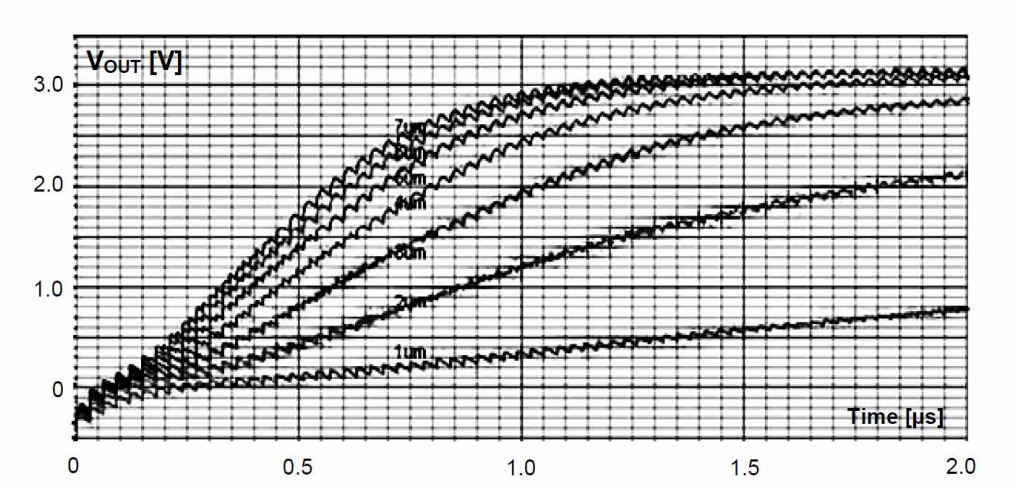

Fig. 5. Output voltage from the charge pump against time and channel width of the switching transistors.

2.2. Ring oscillator

The oscillator generating switching signals for the main charge transferring transistors was made of a few CMOS inverters connected to form a ring (Fig. 6).

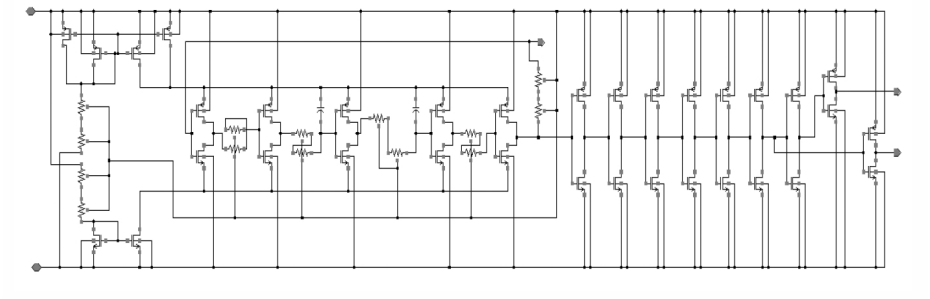

Fig. 6. Scheme of the ring oscillator.

The lower the oscillator frequency the lower power consumption was achieved, but on the other hand also the output voltage level was decreasing. So, the optimal switching frequency should be set between 20-50MHz (Fig. 7).

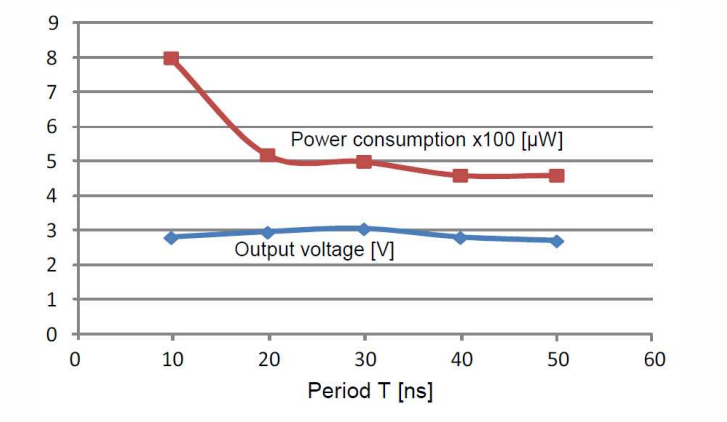

Fig. 7. Output voltage and power consumption against the period of the ring oscillator.

The natural frequency of the oscillator that consisted only of inverters was too high to meet the assumed requirements. To overcome this drawback, some auxiliary current sources were added (Fig. 8) that decreased the charging current and slowed down the rate of charging and discharging the capacitors.

The output of the ring oscillator was next connected to a cascade of inverters forming a square-like signal. Moreover, they play the role of buffers enabling switching of the capacitors between the supplying voltage level and the ground.

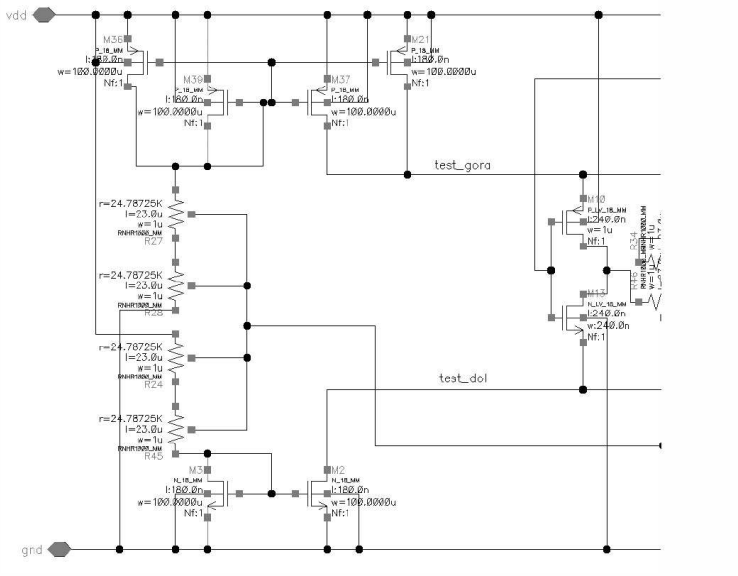

Fig. 8. Scheme of the current source.

In Table 1, the obtained results of calculations illustrating the dependence of the generated period and dissipated power of the internal oscillator, on the supplying voltage are shown.

Table 1. Influence of the supplying voltage on generated period and dissipated power in the internal oscillator.

Voltage [V]	Period [ns]	Dissipated Power [µW]
1	46	52
0,9	49	47
0,8	53	36
0,7	59	28
0,6	72	21
0,5	97	15

2.3. Complete layout of the voltage converter

The capacitors for storing and switching the electrical charge are the crucial parts of each charge pump. In our case, to implement the capacitors on the silicon die there should be some kind of trade-off between available power as well as output voltage and on the other hand the capacitance of the capacitors. A simulation example for the used technology was performed and the results are depicted in Fig. 9. With increasing capacitance also the output voltage and the output power become greater.

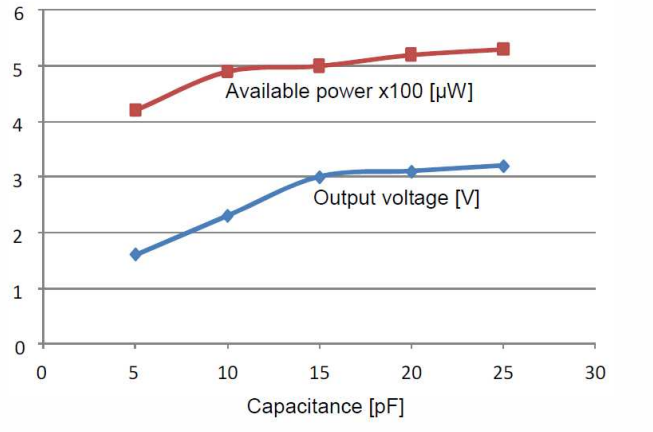

Fig. 9. Output voltage and available power against capacitance.

To meet the project objective, we set the capacitance to a value corresponding to the required output voltage. So, the capacitors were designed as 1,5pF blocks connected in parallel by ten in a row. The final version of the complete ASIC is shown in Fig. 10.

As could be expected the capacitors of the charge pump occupied most of the silicon die of the ASIC (87,5%), the least area (0,3%) was dedicated to the core of the charge pump consisting of pMOS switches and inverters. The remaining silicon area of the die was devoted

to the ring oscillator. The detailed percentage of the each functional block of the chip is shown in Table 2.

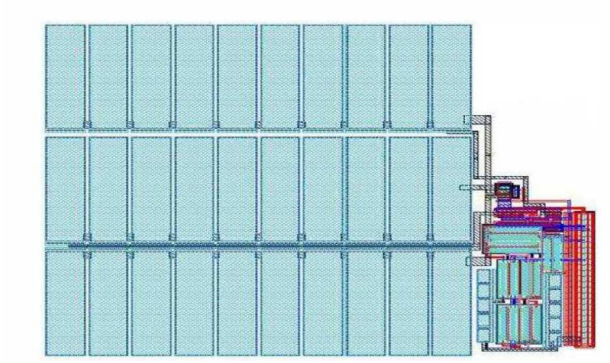

Fig. 10. Layout of the complete circuit for voltage conversion.

Table 2. Silicon die occupation by individual parts of the ASIC.

Part	**Dimensions [µm x µm]**	**Silicon die occupation [%]**
Charge pump	13 x 15	0.3
Ring oscillator	60 x 108	12.2
Capacitors	215 x 216	87.5
Complete ASIC	245 x 216	100

2.4. Post-layout simulations

During a series of post-layout simulations different scenarios of the charge pump operation were examined, among others the output voltage and available power against load current and input voltage were investigated. Fig. 11 shows the results of real-circuit simulations with the internal oscillator integrated on the same silicon die.

For comparison, in Fig. 12 the same output voltage from the charge pump is shown but in the case of an external switching generator. The simulations prove how the built-in oscillator degrades the parameters of the voltage converter.

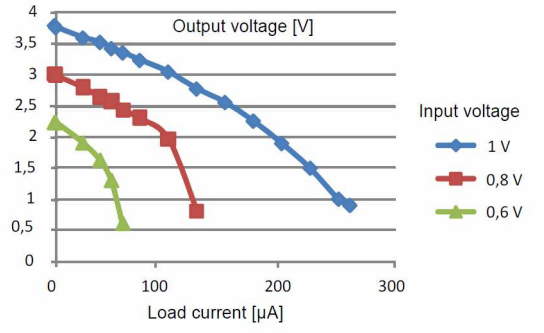

Fig. 11. Simulations of the output voltage from the charge pump (with internal oscillator) against load current and input voltage.

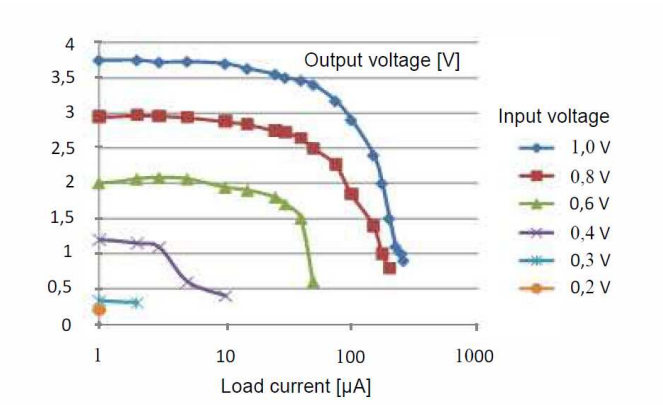

Fig. 12. Simulations of the output voltage from the charge pump (with external oscillator) against load current and input voltage.

The simulations of the available power from the converter with the internal as well as the external oscillator are shown in Fig. 13. All the results confirm the design assumptions, for example for an input voltage V_{IN}=1V and current load I_L=100µA the output voltage was V_{OUT}=3V. The estimated dissipated power was equal to 220µW in case of 520µW delivered by the TEG. During simulations it appeared that the input threshold voltage that determines the starting point of the charge pump was equal to 0,6V, the maximum output power was then 65µW and the output voltage V_{OUT}=1,63V for a current load of I_L=40µA.

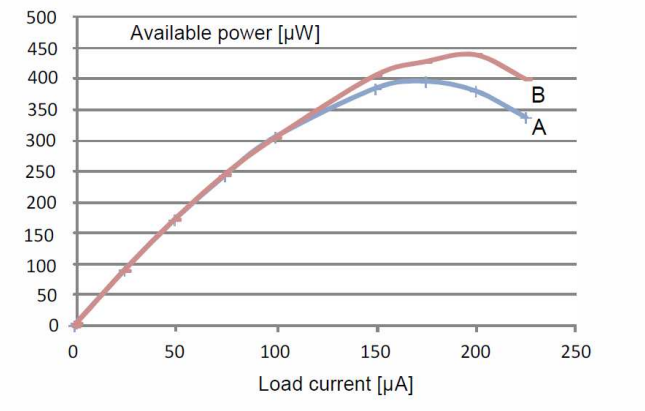

Fig. 13. Available power from the charge pump for input voltage V_{IN}=1V: A- with internal oscillator, B- with external switching generator.

The operation of the converter relies on continuous pumping of the electrical charge from the input to the output. Periodicity of the charge transfer causes that some voltage ripple appears at the output. Its magnitude depends on the load current level and it has an increasing tendency. Results of simulations of the output voltage ripple are shown in Fig. 14. Depending on whether the simulations were performed in relation to a version with built-in oscillator or not, the amplitude of voltage ripple is close to the 0,1V level, which gives 3,3% distortion of the output DC voltage.

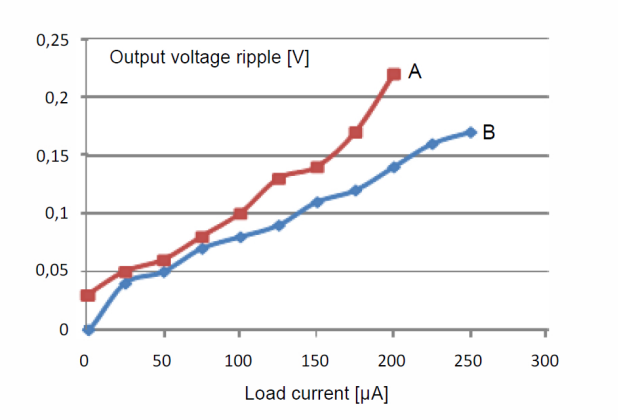

Fig. 14. Output voltage ripple from the charge pump: A- with internal oscillator, B- with external switching generator.

3. Conclusions and future work

Although the output voltage from a TEG is proportional to a temperature gradient, it depends also on the temperature range the thermoelectric module is operating in. It is due to the nonlinear temperature function of the Seebeck coefficient. For instance, for common 40x40mm^2 off-the-shelf Peltier modules and for room temperatures the output voltage of about 600mV results from a 42^o temperature gradient, whereas in the range of 100^{o}C temperatures the only half of that (21^o) gives the same voltage. That is why the presented ASIC is rather intended to be used for harvesting waste heat in an industrial environment with relatively high temperature sources.

After some modifications that are shown in Fig. 15, the designed charge pump could be used in ultra-low-voltage applications and small temperature gradients. By means of a switched transformer with 1:n ratio and a rectifier it is possible to convert even as low as 10mV voltages resulting from a 1^{o}C gradient, easily achievable even from human body heat. To provide a stabilized output voltage to WSN for very low power from TEG, also a low-drop voltage regulator should be added.

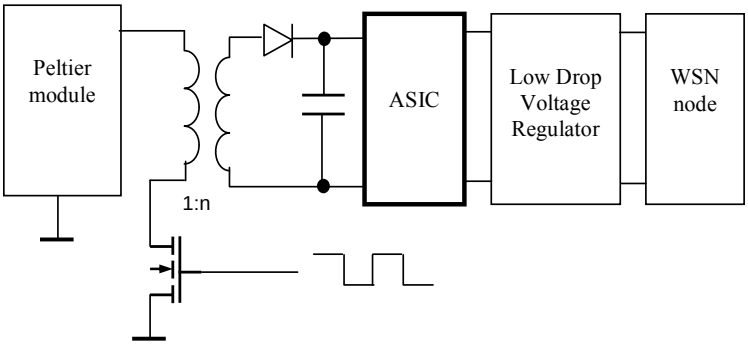

Fig. 15. A modified solution with ASIC for ultralow voltage conversion.

Acknowledgement

The work was supported by the National Centre for Research and Development (NCBiR) project grant No. R02 0073 06/2009.

References

[1] Joseph, A.D. (2005). Energy Harvesting Projects. Published by the *IEEE CS and IEEE ComSoc*. 1536-1268/05.

[2] Mateu, L., Codrea, C., Lucas, N., Pollak, M., Spies, P. (2006). Energy Harvesting for Wireless Communication Systems Using Thermogenerators. At *www.iis.fraunhofer.de/fhg/Images/mateu_et_al_fv_dcis2006_tcm97-73301.pdf.*

[3] Dziurdzia, P. (2009). Modeling of Energy Harvesting Processes in Thermoelectric Modules. In *Proceedings of the XXXIII-rd International Conference of IMAPS-CMPT IEEE Poland*. Pszczyna, 104-110.

[4] Mirocha, A., Dziurdzia, P. (2008). Improved electrothermal model of the thermoelectric generator implemented in SPICE. In *Proc. Of the International Conference on Signals and Electronic Systems*. Cracow, Poland, 317-320.

[5] Beeby, S., White, N. (2010). *Energy Harvesting for Autonomous Systems.* Artech House 2010.

[6] Priya, S., Inman, D.J. (2009). *Energy Harvesting Technologies.* Springer 2009.

[7] Bhalerao, S.A., Chaudhary, A.V., Patrikar, R.M. (2007). A CMOS Low Voltage Charge Pump. In *Proceedings of the 20th International Conference on VLSI Design and 6th International Conference on Embedded Systems.* Bangalore, 941-946.

[8] Choosing the Right RS-232 Transceiver. At http://www.maxim-ic.com/app-notes/ index.mvp/id/2020.

[9] Gregoire, B.R. (2006). A Compact Switched-Capacitor Regulated Charge Pump Power Supply. In *IEEE Journal of Solid-State Circuits*, 41(8), 1944-1953.

[10] Tanzawa, T., Tomoharu, T. (1997). A Dynamic Analysis of the Dickson Charge Pump Circuit. In *IEEE Journal on Solid-State Circuits*, 32(8), 1231-1240.

[11] Zhang, M., Llaser, N. (2003). Dynamic analysis of Dickson charge pump circuits with a resistive load. In *Proceedings of the 2003 10th IEEE International Conference on Electronics, Circuits and Systems*.

[12] Starzyk, J.A., Ying-Wei, Jan, Fengjing, Qiu. (2001). A DC–DC Charge Pump Design Based on Voltage Doublers. In *IEEE Transactions on Circuits and Systems I: Fundamental Theory and Applications.* 48(3), 350-359.

[13] Ahmadi, M., Jullien, G. (2005). A New CMOS charge pump for low voltage applications. In *Proceedings of IEEE International Symposium on Circuits and Systems ISCAS*. 4261-4264.